

2nd Conference on Production Systems and Logistics

Experimental Validation Of A Solidification Model For Automated Disassembly

Richard Blümel¹, Annika Raatz¹¹ Leibniz University Hannover, Institute of Assembly Technology, An der Universität 2, 30823 Garbsen, Germany

Abstract

Disassembly is a crucial step towards sustainable life cycle engineering. During the operation, assembly connections solidify to an unknown state, e.g. due to thermal or mechanical stress on the product. Therefore, disassembly forces are hard to predict. With regard to automated disassembly, this complicates the proper planning of disassembly times and tools. The uncertainties can lead to damage or destruction of the product, impeding regeneration. To tackle these problems, in earlier work, we proposed a solidification model, which enables planners to predict disassembly forces based on the products geometric properties and operational history without investigating the complex physical influences caused by the usage of the product. The disassembly of high-value capital goods like aircraft engines, in particular blade-disk connections, serves as an application case. Still, we were not yet able to validate the solidification model due to the lack of experimental reproducibility. In this work, we adapt the existing model of a solidified assembly connection created in prior work with an additional clamping force. The additional force aims to represent the solidification force. This can significantly increase reproducibility and reduce disturbances.

Keywords

Disassembly; Regeneration; Turbine Blades; Design of Experiments; Regression Model

1. Introduction

Disassembly is a process that is strongly characterized by uncertainties [1]. In contrast to assembly, essential process variables to plan an automated process such as the force to be applied and the duration of the process can only be estimated based on experience and cannot be determined precisely [2]. During operation, products are subjected to physical and thermal stress or corrosion. Thus properties, such as joining tolerances, used to plan assembly lose their validity. This way, detachable connections solidify into hardly or even non-detachable connections, resulting in unknown disassembly planning parameters. The Collaborative Research Centre (CRC) 871, "Regeneration of Complex Capital Goods", aims to develop a scientific basis for maintenance, repair and overhaul (MRO) using aircraft engines high-pressure turbine (HPT) blades as the focus of attention. The expenses for MRO of aircraft engines cause approximately one-third of the engine's operation costs [3]. New turbine blades can cost as much as \$8,000 each [4], making regeneration appropriate. The main goal of the research within the CRC 871 is to restore or even improve the functional properties to save and regenerate as many worn components as possible.

One aspect of the CRC 871 is establishing a projectable disassembly procedure of the HPT blades out of the turbine disks as the initial step for regeneration. Usually, qualified and skilled workers mainly carry out the disassembly based on practical knowledge due to the difficulty of predicting process parameters [5]. However, the vague condition of turbine blades still carries the risk of further damage. That can lead not only to delays but also to parts becoming unusable for regeneration. As a result, it becomes difficult to predict

and plan the disassembly time, and all subsequent regeneration processes cannot be efficiently scheduled. In order to plan and establish an automated disassembly process, it is necessary to gain information concerning parameters affecting the turbine's state. One of the main parameters is the solidification, which directly influences the disassembly force and time. In prior work, we developed a model to determine the force to disassemble aircraft engine turbine blades by simulation and experimental investigation [6][7]. Since we could not use real solidified samples of a used aircraft turbine, we create the solidified samples synthetically. The simulation and following experimental investigation so far were altogether valuable but were missing reproducibility. To face that deficit, in this work, we adapt the model with an additional variable, which represents the solidification and which we can adjust actively. Additionally, this paper aims to validate the applicability of the solidification model using replicated samples. The goal is not to exactly emulate real turbine blade disassembly but to create a basis for further experimental investigation and a method to evaluate different disassembly strategies. First, we briefly describe the existing approaches in chapter 2. In chapter 3, we will present the disassembly test rig used for our experiments, which we use to validate the solidification model described in chapter 4. Last, we will give a conclusion as well as an outlook in section 5.

2. Related Work

During operation, numerous influences change the condition of aircraft engines. The variation of flight routes, e.g. over desert or ocean, hours of operation or number of cycles, and the construction differences like material or geometry make it challenging to know in what manner the assembly connections solidify. Especially hot corrosion, caused by a mixture of components in the fuel and the intake air (e.g. sand, sea salt), is the determining factor for changing the surface's structure [8]. This not only weakens the components but also increases the effort required for disassembly. As introduced, the focus is on the disassembly of HPT blades, whose assembly connection solidify from a clearance fit during assembly to an unknown state. Process parameters like the disassembly force or time become unpredictable, which hinders the automation of disassembly. Therefore, skilled workers generally perform the disassembly manually, *inter alia*, using hammer strikes. However, this carries the risk of further damage.

While the automated disassembly of consumer goods like electronics [9] or electric vehicle's batteries [10] is currently widely researched, the automated disassembly of complex capital goods like aircraft engines is yet barely investigated. In order to plan and automate the disassembly of turbine blades, we plan to determine and predict disassembly parameters based on the solidification caused by wear and tear due to operation. Research on determining aircraft engine's maintenance intervals showed the possibility of predicting the remaining lifetime of turbine engine parts [11]. In prior work, we developed a model of an operationally solidified turbine-blade-disk connection to determine the disassembly parameters [6]. Using that model, we created a learning method to predict disassembly parameters based on known operational influences like hours of operation or flight routes, e.g. desert or ocean [12]. Also, we investigated decoupling the disassembly parameters from the assembly connection's geometry [7]. Using our developed technique, we intend to transcribe disassembly parameters like the force of a well-investigated geometry "A" to a yet-unknown geometry "B" without measuring it beforehand. Thus, it is no longer necessary to examine each geometry individually. Instead, we can include the geometric properties in the prediction of disassembly parameters.

2.1 Development Of A Solidification Model

Figure 1 shows the model's development, starting with an exemplary turbine disk with turbine blades inserted in a slot with a fir-tree shape in a) and a cut along the intersection line through the blade root in a turbine disk in b). Figure 1c) shows the solidification model. The solidifying force $F_s(z)$ is the force resulting from the solidification that must be exceeded by the disassembly force F_{DM} of the tool. The weight force of the blade root sample supports the disassembly force. The contact surface $A_{CS}(z)$ can be taken from CAD data

and decreases during the disassembly process along the disassembly path z . It will become zero when the actual path z reaches the total disassembly length l_D . A modelled interference fit between the blade root and the turbine disk represents the solidification, where the resulting surface pressure p is the central solidifying characteristic.

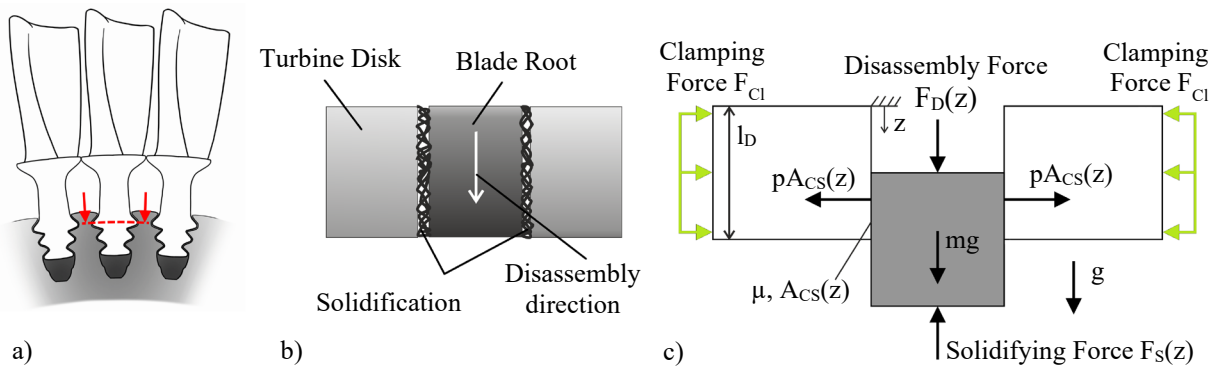


Figure 1: a) Cut through the Turbine Disk, b) Sectional view of the Turbine Disk, c) Solidification model [7]

To use the model for analysis, we transferred the model into a FEM-simulation. The simulation showed the possibility of defining and calculating constant parameters for each geometry. These geometry parameters can then be used to compare disassembly forces of two blade root shapes with a similar usage history [7]. To verify the simulation, we conducted several experiments. As aforementioned, the experimental investigation would require used aircraft turbines, which we do not have. Therefore, we had to create operational solidified disk-blade connections synthetically.

2.2 Previous Approaches For Synthetic Solidification Modeling

The first attempt was to rust samples of a blade-disk connection artificially. They consisted only of the blade root and a surrounding segment of the turbine blade. We designed three different kinds of shapes to investigate the geometry's transferability. They were similar to the fir-tree-design (Figure 1a) but with an upscaled size, consisting of an inner part, the replica blade-root, and an outer part, the replica turbine disc. The samples were made of mild steel so that they rust easily. We also specified a clearance fit so that a disassembly force in the non-solidified state is zero, just like the original connection. To artificially induce solidification, we left samples to rust in a salt spray chamber. The following disassembly test's results showed that disassembly was hardly possible. We could see wildly varying degrees of rust covering the samples. Furthermore, we could only use every probe only once for disassembly testing. Thereby the tests lack reproducibility and even feasibility. They also require a considerable amount of samples to repeat.

The second approach synthetically emulating an operational solidified blade-disk connection was to add industrial glue onto the contact surfaces of similar samples. We let it harden with varying contact pressure and times. Using an adhesive remover, we were now able to clean and therefore reuse the sample. However, compared to the rust tests, we could see much lower disassembly forces. Beyond that, we saw a very high variation in the test results. We also observed a visibly recognizable unequal glue distribution between the left and the right side and along with the shape itself. Summarily, we get a better reproducibility since we can repeat the tests more often, but we see a higher variation in the results due to the manual glue application process.

The experiments show that they lack reproducibility and are subject to variations by human inaccuracy. To tackle these obstacles, we adapt the existing solidification model. Instead of synthetically creating solidified connections, we add the clamping force F_{Cl} instead of an interference fit to induce the surface pressure caused to tackle the disadvantages and difficulties (Figure 1c). That allows us to repeat the experiments infinite times and always set the same surface pressure. A clamping unit will apply the external force. To examine

and validate the adapted solidification model, we had to rework the disassembly test rig, described in the following.

3. Disassembly Test Rig

To investigate solidified turbine disk-blade root connections, we developed and built a test rig to perform disassembly tests (Figure 2). The central part is the disassembly unit, consisting of a servo motor, a gearbox, and a ball screw to produce the disassembly tool's speed. It also has a piezo-stack-actuator, a 10 kN load cell to measure the disassembly force and a pushing rod. The piezo-stack-actuator is not relevant for this paper and will be used in future work to reduce the disassembly force using micro impacts. Since the piezo actuators maximum load is 4.5 kN, the disassembly is limited to this force. The second and new element of the test rig is the clamping device to model a solidified assembly connection. The clamping unit consists of another servo motor with an integrated gearbox connected to a machine vice with a maximum force of 45 kN. Both are placed on a plain linear guidance to position the sample holder under the disassembly pushing rod manually. The sample mount is placed between the vice's jaws and includes another load cell with a maximum force of 50 kN. The samples are placed and clamped with repeatable accuracy using a locking pin and an adjusting screw. By setting the clamping force, the samples placed between the clamping unit's jaws represent a solidified turbine disk-blade connection with a reproducible degree.

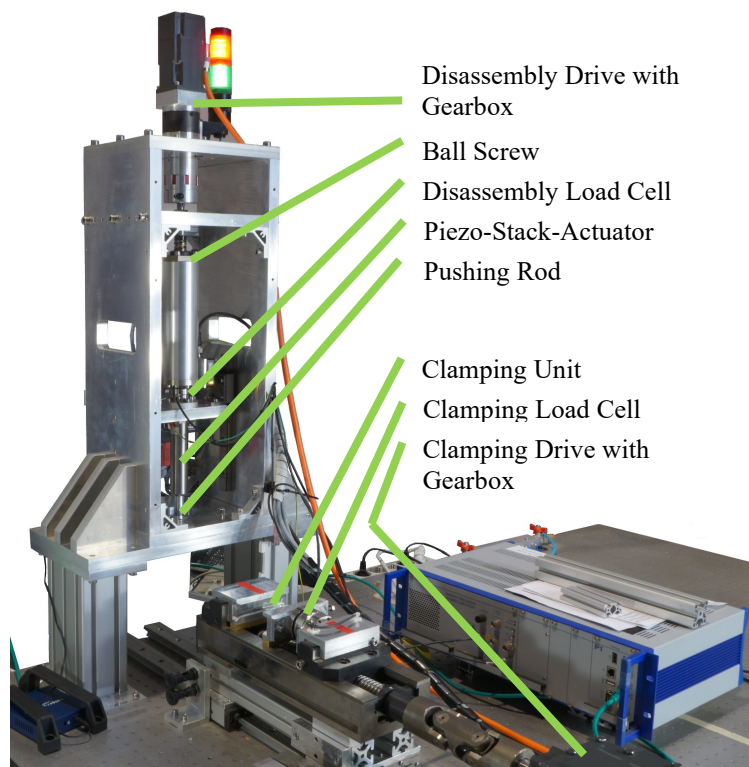


Figure 2: Turbine Blade Disassembly Test Rig

The entire system has been integrated with a Siemens PLC. With a mobile HMI panel, we can control the test rig. We use the gear transmission ratio of the gearbox and the thread pitch of the ball screw to calculate the disassembly speed from the motor's revolution speed. A laser distance sensor measures the path and determines the actual feed. To clamp the samples, we set the desired clamping force, and the servo motor turns the vice's spindle until the set value is reached. Using the PLC's internal data logging function, we can record the parameters time, disassembly speed, clamping force, distance and disassembly force. This allows us to collect the necessary data during the experiments.

4. Validation of the Solidification Model

In order to examine and validate the applicability of the solidification model, we will use the Design of Experiments (DoE), which is a technique to resolve usually complex and costly experiments efficiently. With all influences and factors included, we can obtain maximum information with a given number of experiments [13]. DoE also normalizes the data to assist the investigation and finds the values of significant factors and those with little influence. The relationship between the input variables and the effect on the output is evaluated using regression analysis, a curve-fitting method to predict an output or dependant variable based on inputs or independent variables [14]. That allows us to determine whether the variation of disassembly parameters can predict disassembly forces. It also shows the significance and amount of the influence on the output.

4.1 Full factorial DoE Analysis with Three Parameters

We will plan the experimental design by considering the main parameters for disassembly. For a profitable process from an economic point of view, the disassembly time is essential. With the relationship between disassembly path z and the disassembly time, we define the disassembly speed v_D as the first factor. The second factor is the clamping force, which resembles the solidification, as mentioned before. Furthermore, we add a third factor, the shape of the blade root, to investigate the contact surface and geometric form variation. As mentioned before, we want to decouple the disassembly parameters from geometric properties.

We considered the total samples' length of 20 mm and the disassembly time to define the disassembly speed levels of the DoE plan. Thus, we chose 1 mm/s for a slow and 10 mm/s for a fast disassembly speed to push out the blade root. In preliminary tests, we located the lower and upper level for the clamping force. When setting it lower than 2 kN, the probes repeatedly fell down before the actual test, as for higher forces than 8 kN, we were unable to push out the samples. We took the original HPT blade and redesigned two related contours to vary the blade root's shape and the contact surface (Figure 3). The samples are made of stainless steel to prevent them from rusting. Also, stainless steel is less costly than the original CSMX-4 superalloy.

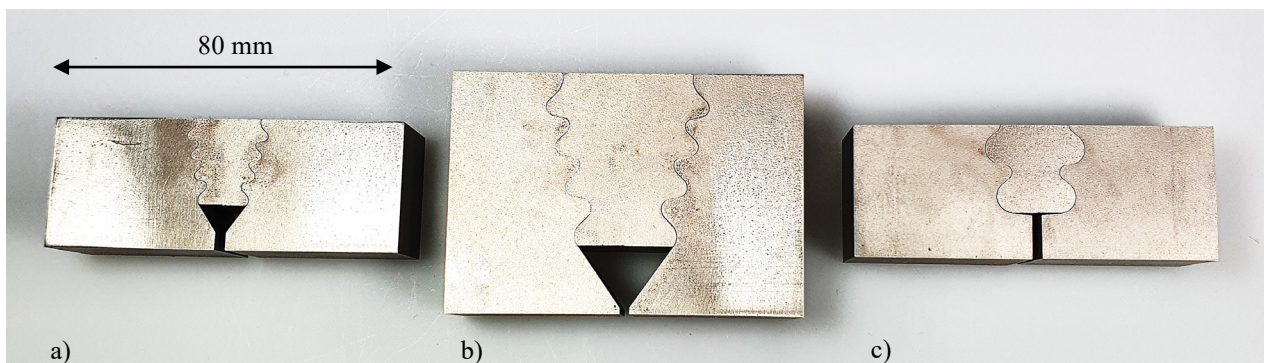


Figure 3: Overview of the different blade root shape samples: a) "Original", b) "Double", c) "B-shape"

We named the original form "Original", a contour twice the size "Double" and a third shape with the same contact surface but a different contour as the original one, "B-shape". In the experimental design, the shape of the blade root has a particular position. We divide it into three levels since it has three categories and is not a continuous variable. The levels for the factors are presented in Table 1.

Table 1: Levels of influential parameters levels in full factorial design

Factors	Low (0)	High (1)	
Disassembly Speed (v_D), mm/s	1	10	
Clamping Force (F_{Cl}), N	2000	7000	
Shape of Blade-Root (BRS), -	Original	Double	B-shape

We use the full factorial experimental design to investigate the three input variables at all possible combinations. That allows us not only to examine the influence of each factor but also the effects of interactions between the factors on the output variable. We conducted every experiment five times. The shown response variable in Table 2 is the mean over five repetitions of the disassembly force, presenting the resulting observations using the mentioned values for each factor of Table 1.

Table 2: Observation table: full factorial design

Run order	v_D	F_{Cl}	BRS	Disassembly Force (N)
1	1	1	Original	2794.51 ± 87.40
2	0	1	Original	2697.25 ± 178.30
3	1	0	Original	761.18 ± 86.63
4	0	0	Original	853.39 ± 52.72
5	1	1	Double	2362.55 ± 259.51
6	0	1	Double	2018.83 ± 207.94
7	1	0	Double	674.40 ± 96.28
8	0	0	Double	594.18 ± 54.88
9	1	1	B-shape	2200.49 ± 235.34
10	0	1	B-shape	2211.12 ± 177.74
11	1	0	B-shape	725.72 ± 122.05
12	0	0	B-shape	776.67 ± 119.38

4.2 Regression Analysis

In order to perform the regression analysis, we create a polynomial for Y, the dependant variable as a function of the explanatory variables X_i . We can also include terms to describe the influence of interdependences. To catch the diversification of the Y values, we need to add a residuum ϵ . With n observations, β_i the partial regression coefficients and two input variables, an exemplary equation for the regression follows to:

$$y_i = \beta_0 + \beta_1 \cdot x_{i,1} + \beta_2 \cdot x_{i,2} + \beta_3 \cdot x_{i,1} \cdot x_{i,2} + \epsilon_i, \quad i = 1, \dots, n \quad (1)$$

In our case, y_i stands for the estimated value for the disassembly force, and the input variables are the disassembly speed, clamping force and the blade root's shape. As mentioned before, the blade root's shape is a categorical variable. Therefore, we need two dummy or binary variables d_1 and d_2 , to analyze the categories, as shown in [15]. Whenever the observation of the blade root's shape is "Double", d_1 is equal to one, otherwise zero. Similarly, we define d_2 as equal to one for "B-shape" and otherwise zero. The original shape will become the reference category since both dummy variables will be equal to zero. That results in Equation 2 for the multiple linear regression.

$$\hat{y} = \beta_0 + \beta_1 \cdot v_D + \beta_2 \cdot F_{Cl} + \beta_3 \cdot v_D \cdot F_{Cl} + \beta_4 \cdot d_1 + \beta_5 \cdot d_2 + \beta_6 \cdot v_D \cdot d_1 + \beta_7 \cdot v_D \cdot d_2 + \beta_8 \cdot F_{Cl} \cdot d_1 + \beta_9 \cdot F_{Cl} \cdot d_2 \quad (2)$$

When observing the original form, d_1 and d_2 are zero, each term containing d_1 and d_2 is dropped. Looking at the "Double" shape, d_1 will be one, and d_2 will stay zero leading to adding β_4 to β_0 , β_6 to β_1 and β_8 to β_3 , and dropping $\beta_5 \cdot d_2$, $\beta_7 \cdot v_D \cdot d_2$ and $\beta_9 \cdot F_{Cl} \cdot d_2$. For "B-shape", it is vice-versa.

Table 3 shows the regression's results for each input variable. The Effect-column shows the effect of changing the factors from low to high, based on each mean value. For example, increasing the disassembly speed from 1 mm/s to 10 mm/s increases the resulting disassembly force by 61.24 N. The Coef-column

shows each regression coefficient β_i , and their standard errors in the SE Coef-column. They can be the same when the design matrix for calculation is orthogonal. It also contains the t-and p-values for the following goodness of fit test. The t-value is the coefficient divided by its standard error. It is used to determine the p-value from the Student's t-distribution and used for testing the significance [16].

Table 3: Coefficients table for disassembly force

Term	Effect	Coef	SE Coef	t	p
Constant		847.13	53.17	15.932	< .001
v_D	61.24	-79.67	67.26	-1.185	0.243
F_{Cl}	1649.87	1856.39	67.26	27.602	< .001
$v_D \cdot F_{Cl}$	1195.54	146.42	67.26	2.445	0.018
d_1	-215.05	-277.72	71.34	-3.893	< .001
d_2	-116.03	-39.43	71.34	-0.553	0.583
$v_D \cdot d_1$	-44.86	209.45	82.37	2.543	0.014
$v_D \cdot d_2$	-111.30	-33.32	82.37	-0.405	0.688
$F_{Cl} \cdot d_1$	761.80	-382.20	82.37	-4.640	< .001
$F_{Cl} \cdot d_2$	779.94	-483.99	82.37	-5.876	< .001

4.3 Goodness of Fit

After collecting all the data and setting up the regression model, we can now check its adequacy and fitting. The most commonly used measure for the "Goodness of Fit" of multiple regression is the multiple coefficient of determination or R^2 [16]. Its limits are between zero and one; the closer to one, the better is the fit. The calculated R^2 for our model is 0.981, as seen in Table 4. The disadvantage of R^2 is that with many input variables, its value can be high, even though one or more inputs do not affect the output. Beyond that, adding more regressors always increases but never decreases R^2 because it assumes that every predictor explains the dependant variable. The adjusted R^2 tackles this problem by considering only those input variables that affect the output. A value for the adjusted R^2 at 0.977 testifies a good fit, too.

Table 4: Regression statistics for full factorial design

Term	Value
Standard error of regression	SER 130.240
Coefficient of determination	R^2 0.981
Adjusted coefficient of determination	Adjusted R^2 0.977

After that, we will test the regression model's overall significance, i.e. test if the source of variation in Y is due to random influences or dependent on the input variables. To do this, we use null hypothesis testing. Each null hypothesis must be rejected to show a dependency between predictor and response variable. If each null hypothesis is rejected, the alternative hypothesis must be true, stating that at least one of the regressors is unequal zero.

The first assumption to investigate whether to accept or reject is the joint hypothesis. It states that all regression coefficients are zero simultaneously, as in Equation 3. We do this by the analysis of variance (ANOVA). To reject the joint hypothesis, the resulting p-value of the ANOVA-procedure must be lower than the significance level α . We chose a level of $\alpha = 0.05$, which means the risk of including effects that have no influence is 5%. A rejection of the null hypothesis will lead to accepting the alternative hypothesis (Equation 4), which states, as mention before, that at least one regressor has predictive power.

$$H_0: \beta_1 = \beta_2 = \dots = \beta_i = 0 \quad (3)$$

$$H_a: \beta_i \neq 0 \quad (4)$$

As seen in Table 5, the calculated p-value is lower than the significance level α , which leads to the rejection of the joint hypothesis that all input variables together have no effect on the disassembly force in the model estimated. This indicates that the regression has predictive power for the disassembly force.

Table 5: ANOVA for full factorial design

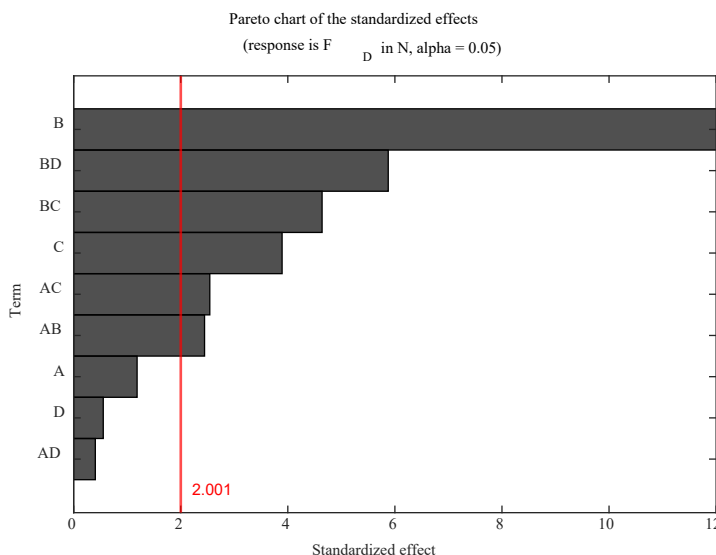
	Degrees of freedom	Sum of Squares	Mean Square	F	p
Regression	9	$4.332 \cdot 10^7$	$4.813 \cdot 10^6$	283.754	< 0.001
Residual	50	$8.481 \cdot 10^5$	$1.696 \cdot 10^4$		
Total	59	$4.417 \cdot 10^7$			

The second hypothesis testing of the regression and the model's usefulness is the significance test for each slope coefficient β_i individually. In this case, the null hypothesis states that the individual regression is not zero, as seen in Equation 5.

$$H_0: \beta_i = 0 \quad (5)$$

$$H_a: \beta_i \neq 0 \quad (6)$$

If a slope's t-value is greater than the critical t-value for the significance level α , the null hypothesis will be rejected. From this follows that the alternative hypothesis is fulfilled, which means that the individual regression coefficient is not zero (Equation 6). As seen in Figure 4, the clamping force and all its interactions are significant, as well as the "Double"-shape's variable and its interactions. However, the disassembly speed, the "B"-shape's dummy variable and their interaction are statistically not relevant, meaning that these terms have such a small impact that they are irrelevant for predicting the disassembly force.



Factor	Name	Unit
A	v_D	mm/s
B	F_{Cl}	N
C	d_1	-
D	d_2	-

Figure 4: Pareto chart of full factorial design for disassembly force

Null hypothesis testing can only be applied for normally distributed estimators β_i . Since they are linear functions of each ε_i , we can test the residual's normal distribution. If the residuals are normally distributed, the estimators are as well. In our analysis, the normal probability plot (Figure 5a) indicates that the normal distribution is a good model for the results but shows a few outliers. The residuals' distribution follows a bell

shape curve and also shows the presence of outliers, as they make it slightly skewed to the left and right, as seen in Figure 5b). We can therefore assume that the residuals are normally distributed, and the null hypothesis testing is valid.

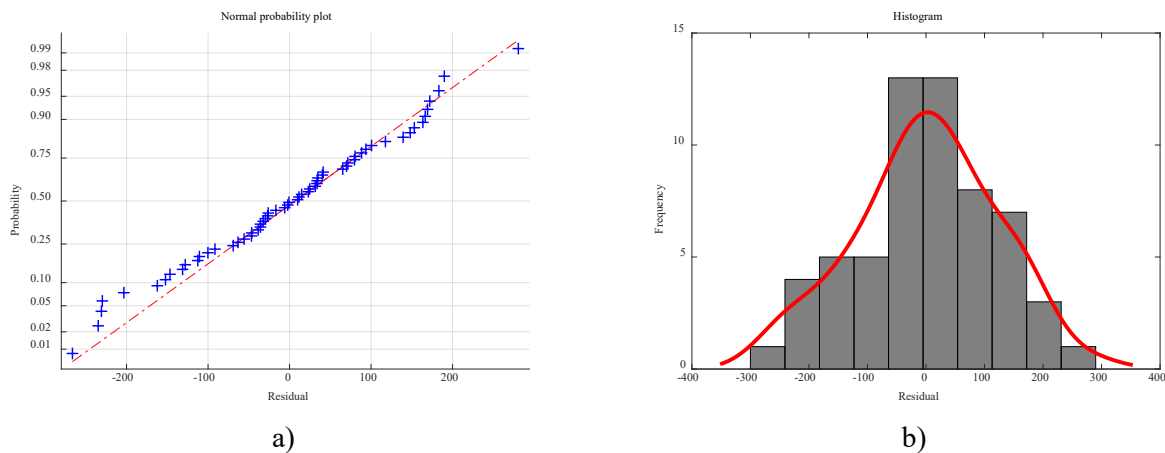


Figure 5: Residual Plots for Disassembly Force: Full Factorial Design

The experiment shows the unexpected result that the disassembly speed has a minor influence on the disassembly force. A tenfold increase in speed from 1 mm/s to 10 mm/s decreases the disassembly force by an average of only approximately 61 N. In contrast, as expected, the clamping force has vast influence. Increasing it by 5 kN increases the resulting disassembly force by around 1.65 kN. The customized geometric shape with twice the contact surface shows a significant influence, too, in contrast to the "B-shape", whose influence can be seen as noise. According to [16], the coefficients' standard error measures its prediction accuracy. In our case, they indicate a relatively good precision. It also shows that the estimation of the input's coefficients is more precise than the dummy variable's and interactions' coefficients.

In summary, the regression analysis is suitable to describe the solidifying model. It can therefore predict the disassembly force based on the predictors speed and clamping force. Furthermore, we can include the geometric shape in the prediction model. The exact dependence of the geometric shape on the output variable and a decoupling from geometric properties will be investigated in future work. Also, we need to determine the correlation between the operational influences (flight route, number of cycles) and the clamping force.

5. Conclusion and Outlook

This work's objective is to adapt the existing solidification model and to validate its applicability. As mentioned at the very beginning, our previous research's main issue was the lack of reproducibility. We showed that we could model a solidified turbine disk-blade joint in a reproducible manner by an additional force using a clamping unit. The experiment was planned using DoE to gather data. With setting up a regression, we created a basis to predict the disassembly force to plan disassembly tools and time based on performed experiments and gathered data. We can also automated disassemble simple turbine blade samples using the disassembly test rig and measure the necessary information to predict the disassembly force.

In future work, we will add the presented piezo-stack-actuator to confirm the possibility to decrease the needed disassembly force, as seen in past investigations. Since the manufacturers instruct specifications and damage patterns for accepting or rejecting parts for reuse, we need to reduce the pressure on the surface as much as possible. Together with the prediction model, we can establish a foundation for an adaptive and component friendly disassembly process. Additionally, we need to investigate how operational parameters like the number of cycles and flight routes affect the modelled solidification. Eventually, we want to use the developed knowledge to predict the disassembly parameters depending on the operation. That will support aviation MRO planners and companies to plan an automated and component friendly disassembly efficiently.

Acknowledgements

Funded by the Deutsche Forschungsgemeinschaft (DFG, German Research Foundation) – SFB 871/3 – 119193472

References

- [1] Lambert, A.J.D., 2003. Disassembly sequencing: A survey. *International Journal of Production Research* 41 (16), 3721–3759.
- [2] Das, S.K., Naik, S., 2002. Process planning for product disassembly, *International Journal of Production Research* Vol. 40:6, pp. 1335-1355.
- [3] Rupp, O., 2001. Instandhaltungskosten bei zivilen Strahltriebwerken, *Deutscher Luft- und Raumfahrtkongress 2001*, DGLR-2001-008, Hamburg
- [4] Ackert, S., 2011. Engine Maintenance Concepts for Financiers, Technical Report, Aircraft Monitor
- [5] Tao, W. Huapeng, D., Jie, T., Hao, Wa., 2015. Recent Repair Technology for Aero-Engine Blades, *Recent Patents on Engineering* Vol. 9, No 2, pp. 132-141.
- [6] Wolff, J., Yan, M., Schultz, M., Raatz, A., 2016. Reduction of Disassembly Forces for Detaching Components with Solidified Assembly Connections, *Procedia CIRP* 44, pp. 328-333.
- [7] Wolff, J., Kolditz, T., Fei, Y., Raatz, A., 2018. Simulation-Based Determination of Disassembly Forces, *Procedia CIRP* 76, pp. 13-18.
- [8] Betz, W., Huff, H., Track, W., 1976. Zur Bewertung von Schutzschichten gegen Heißgaskorrosion an Gasturbinenschaufeln. *Mat.-wiss. u. Werkstofftech.* 7 (5), 161–166.
- [9] Vongbunyong, S., Kara, S., Pagnucco, M., 2013. Application of cognitive robotics in disassembly of products. *CIRP Annals* 62 (1), 31–34.
- [10] Wegener, K., Chen, W.H., Dietrich, F., Dröder, K., Kara, S., 2015. Robot Assisted Disassembly for the Recycling of Electric Vehicle Batteries. *Procedia CIRP* 29, 716–721.
- [11] Müller, M., 2013. Untersuchungen zum Einfluss der Betriebsbedingungen auf die Schädigung und Instandhaltung von Turboluftstrahltriebwerken, Institut für Luftfahrtantriebe, Universität Stuttgart
- [12] Wolff, J., Kolditz, T., Raatz, A., 2019. A Learning Method for Automated Disassembly, *Precision Assembly in the Digital Age*, IPAS 2018, Springer, Cham, vol 530, pp. 63-71.
- [13] Guthrie, W.F., 2020. *NIST/SEMATECH e-Handbook of Statistical Methods* (NIST Handbook 151)
- [14] Toutenberg, H., 2006. *Arbeitsbuch zur deskriptiven und induktiven Statistik*, Springer, Berlin, pp. 227-239.
- [15] Allen, T. T., 2019. *Introduction to Engineering Statistics and Lean Sigma*, Second Edition, Springer, London, pp. 397-401.
- [16] Gujarati, D. N., Porter, D. C., 2008. *Basic Econometrics*, Fifth Edition, Irwin/McGraw-Hill, New York

Biography

Richard Bluemel (*1987) studied mechatronics engineering at Leibniz University Hannover. He was employed at International Automotive Components Group (IAC) as a construction engineer in the field of special mechanical engineering (2014-2019) before returning to the Leibniz University Hannover as a research associate at the Institute for Assembly Technology (match).

Annika Raatz (*1971) has been the head of the Institute of Assembly Technology (match) since its establishment in 2013. Prof. Dr.-Ing. Annika Raatz is a member of the Society for Assembly, Handling and Industrial Robotics (MHI) and the Academic Association for Production Technology (WGP). Her main research topics are robot-aided handling processes, machine concepts for handling, assembly and production automation and soft material robotic systems.